

# Training Robust Deep Neural Networks via Adversarial Noise Propagation

Aishan Liu,<sup>§</sup> Xianglong Liu,<sup>§\*</sup> Chongzhi Zhang,<sup>§</sup> Hang Yu,<sup>§</sup>  
Qiang Liu<sup>†</sup> and Junfeng He<sup>‡</sup>

<sup>§</sup>State Key Laboratory of Software Development Environment, Beihang University, China

<sup>†</sup>Computer Science, University of Texas at Austin, USA

<sup>‡</sup>Google Research, USA

{liuaishan, xlliu, chongzhizhang, hyu0829}@buaa.edu.cn, lqiang@cs.utexas.edu, junfenghe@google.com

## Abstract

Deep neural networks have been found vulnerable to noises like adversarial examples and corruption in practice. A number of adversarial defense methods have been developed, which indeed improve the model robustness towards adversarial examples in practice. However, only relying on training with the data mixed with noises, most of them still fail to defend the generalized types of noises. Motivated by the fact that hidden layers play a very important role in maintaining a robust model, this paper comes up with a simple yet powerful training algorithm named *Adversarial Noise Propagation* (ANP) that injects diversified noises into the hidden layers in a layer-wise manner. We show that ANP can be efficiently implemented by exploiting the nature of the popular backward-forward training style for deep models. To comprehensively understand the behaviors and contributions of hidden layers, we further explore the insights from hidden representation insensitivity and human vision perception alignment. Extensive experiments on MNIST, CIFAR-10, CIFAR-10-C, CIFAR-10-P and ImageNet demonstrate that ANP enables the strong robustness for deep models against the generalized noises including both adversarial and corrupted ones, and significantly outperforms various adversarial defense methods.

## Introduction

Recent advances in deep learning have achieved remarkable successes in various challenging tasks, including computer vision (Krizhevsky, Sutskever, and Hinton 2012), natural language processing (Bahdanau, Cho, and Bengio 2014) and speech (Hinton et al. 2012). In practice, deep learning has been routinely applied on large-scale datasets, where data collected from daily life inevitably contain lots of noises including adversarial examples and corruption (Szegedy et al. 2013; Goodfellow, Shlens, and Szegedy 2014). Unfortunately, such noises are unprevailing to human beings, but misleading to deep neural networks, which pose potential security threats for practical machine learning applications in both digital and physical world (Papernot et al. 2016; Liu et al. 2019).

In the past few years, how to train robust deep neural networks against the noises has attracted great attentions.

The most successful progress lies in developing different adversarial defense strategies (Xie et al. 2018; Dhillon et al. 2018) against adversarial examples. These methods often supply adversaries with non-computable gradients to avoid common gradient-based adversarial attacks. However, Athalye, Carlini, and Wagner argued that most of them only pose a false sense of safety. They circumvent the obfuscated gradients and achieve nearly 100% attacking success rates. Whereas, *adversarial training* (Szegedy et al. 2013) survives it by augmenting training data with adversarial examples. However, though adversarially trained deep models (Alexey, Ian, and Samy 2017) are robust to some single-step attacks, they are still vulnerable to iterative attacks. More recently, Yan, Guo, and Zhang proposed to improve adversarial robustness via integrating an adversarial perturbation-based regularizer into the classification objective.

Beside the adversarial examples (Xie et al. 2018; Cisse et al. 2017), corruption noises such as snow, blur, and other novel combinations also frequently occur in real world, which also bring critical challenges for building strong deep learning models. Dodge and Karam found that deep learning models behave distinctly subhuman to input images with Gaussian noises. Zheng et al. proposed stability training to improve model robustness against noises only confined to JPEG compression. More recently, Hendrycks and Dietterich first established a rigorous benchmark to evaluate image classifier robustness to 75 different corruption noises.

Despite the progress, till now there are rare studies devoted to improving model robustness against corruption, and most existing adversarial defense methods still remain vulnerable to the generalized noises, mainly due to the simple training paradigm by adding adversarial noises to the input data. It is well-known that, in deep neural networks the influence of invasive noises to the prediction can be directly reacted in the sharp variations in the middle feature maps during the forward propagation (Liao et al. 2018; Cisse et al. 2017). Prior studies (Cisse et al. 2017) have proven the fact that hidden layers play a very important role in maintaining a robust model. In (Cisse et al. 2017), adversarially robust models can be promised through constraining the Lipschitz constant between hidden layers, e.g., linear and convolutional layers, to be smaller than 1. Ilyas et al. gener-

\*Corresponding author

ated robust features with the help of penultimate layer of a classifier, which in turn help training a robust model. More recently, Santurkar et al. also noticed the importance of robust feature representation and uses them to deal with many computer vision tasks. This indicates that the noise resistance of hidden layers also plays an important role in training a robust model. Based on the fact, we can directly draw insight from robust hidden representations and build strong deep models by obtaining robust hidden layers during training.

In this paper, we propose a simple but very powerful training algorithm named *Adversarial Noise Propagation* (ANP) to enable the strong robustness for deep models against generalized noises including both adversarial examples and corruption. It injects adversarial noises into the *hidden layers* of neural networks during training, instead of the input in traditional adversarial defense methods. This can be efficiently accomplished by a simple modification of standard backward-forward propagation, without introducing significant computation overhead. Because the adversarial noises from hidden representations are considered during training, models trained by ANP are expected to be more robust against more types of noises, including both adversarial examples and corruption. We also try to give insights of the contributions and behaviors of hidden layers during training from the views of hidden representation insensitivity and human vision perception alignment.

Extensive experiments under both blackbox and whitebox settings on MNIST, CIFAR-10 and ImageNet are conducted to demonstrate that ANP achieves excellent results compared to the common adversarial defense algorithms including the *NeurIPS 2017* adversarial defense winning methods against various adversarial attacks. Meanwhile, experiments on CIFAR-10-C and CIFAR-10-P (Hendrycks and Dietterich 2019) prove that ANP can enhance strong corruption robustness for deep models as well. More evaluation further proves that ANP supplies models with strong robustness against generalized noises.

## Preliminaries

### Terminology and Notation

Given a dataset  $D$  with feature vector  $x \in \mathcal{X}$  and label  $y \in \mathcal{Y}$ , the deep supervised learning model tries to learn a mapping or classification function  $F: \mathcal{X} \rightarrow \mathcal{Y}$ . Specifically, in this paper we consider the visual recognition problem.

### Adversarial Example

Given a network  $F_\theta$  and an input  $x$ , whose ground truth label is  $y$ , an adversarial example  $x^{adv}$  is an input such that

$$F_\theta(x^{adv}) \neq y \quad \text{s.t.} \quad \|x - x^{adv}\| < \epsilon,$$

where  $\|\cdot\|$  is a distance metric to quantify the semantic distance between the two inputs  $x$  and  $x^{adv}$  is small enough. Whereas, adversarial example makes the model predict wrong label, namely  $F_\theta(x^{adv}) \neq y$ .

## Corruption

Image corruption is random variation of brightness or color information in images, such as Gaussian noise, Defocus blur, Brightness, etc., and is commonly witnessed. Supposing, we have a set of corruption functions  $C$  in which each  $c(x)$  performs a kind of corruption function. Thus, average-case model performance on small, general, classifier-agnostic corruption define model corruption robustness:

$$\mathbb{E}_{c \sim C} [P_{(x,y) \sim D} (F(c(x)) = y)].$$

To sum up, corruption robustness measures the classifier's average-case performance on corruption  $C$ , while adversarial robustness measures the worst-case performance on small, additive, classifier-tailored perturbations.

## Proposed Approach

Now we introduce our proposed approach *Adversarial Noise Propagation* (ANP).

### Adversarial Formulation

In the deep neural networks, the sharp variations in the hidden layers will propagate to the later layers and lead to the undesired predictions in practice. Therefore, enhancing the noise insensitivity and guaranteeing the stable behavior in hidden layers will help promise a robust model. In order to obtain a robust model against small noises, we are motivated to improve the ability of layer-wise noise resistance in the deep learning models.

Intuitively, we attempt to add adversarial noises to each hidden layer of a deep learning model by propagating backward from the adversarial loss during training, instead of only manipulating the input layer in traditional adversarial defense methods. This strategy forces the model to minimize the model loss for a specific task, with the opposite adversarial noise in each hidden layer that expects to maximize the loss. Subsequently, the learnt parameters in each layer enable the model to keep consistent and stable predictions for the clean instance and its noisy surrogates distributing in the neighborhood, and thus in turn pose strong robustness for deep models.

Formally, recall that a deep neural network  $y = F(x; \theta)$  as a composition of a number of nonlinear maps, each of which corresponds to a layer:

$$z^{m+1} = f(z^m; \theta), \quad m = 0, \dots, M,$$

with  $z^0 = x$  denotes the input,  $z^M = y$  the output, and  $z^m$  the output of the  $m$ -th hidden layer. Here  $\theta$  collects the weights of the network.

In our framework, we introduce an adversarial noise  $r^m$  on the hidden state  $z^m$  at each layer:

$$z^{m+1} = f(z^m + r^m, \theta), \quad m = 0, \dots, M.$$

We use  $\tilde{y} = F(x; \theta, \delta)$  to denote the final network output with the injected noises  $r = \{r^m\}_{m=0}^M$  at all the layers. We then learn the network parameter  $\theta$  by minimizing the following adversarial loss:

$$\min_{\theta} \mathbb{E}_{(x,y) \sim D} \left[ \max_r \left( L(y, F(x; \theta, r)) - \frac{\eta}{2} \|r\|_2^2 \right) \right], \quad (1)$$

where for each data point  $(x, y)$ , we search for an adversarial noise  $r$ , subject to an L2 norm constraint. The coefficient  $\eta$  controls the magnitude of the adversarial noise.

## Noise Propagation

The key challenge of this framework is obviously solving the inner maximization for individual input data points. This is efficiently addressed in our *Adversarial Noise Propagation* (ANP) by performing gradient descent on  $r$ , with a natural backward-forward style training that adds minimum computational cost over the standard back propagation. This induces the noises propagation across layers and noise injection into hidden layers during the backward-forward training.

Specifically, in each iteration, we first select a minibatch of training data. For each data point  $(x, y)$  in the minibatch, we approximate the inner optimization by running  $k$  steps of gradient descent to utilize the most information in each mini-batch, and fit the data distribution better. Initializing at  $r^{m,0} = 0$  for all  $m = 0, \dots, M$ , we have the adversarial gradient for the  $m$ -th hidden layer  $z^m$ :

$$g^{m,t} = \nabla_{r^m} L(y, F(x; \theta, r^t)) = \nabla_{z^m} L(y, F(x; \theta, r^t)),$$

where we draw the key observation that the gradient of the adversarial noise  $r^m$  equals the gradient of the hidden states  $z^m$ , which is already calculated in the standard backward propagation, hence introducing no additional computations.

Specifically, the noise gradient is calculated recursively during the standard backward propagation:

$$\begin{aligned} g^{m-1,t} &= \frac{\partial L(y, F(x; \theta, r))}{\partial z^{m-1,t}} \\ &= \frac{\partial L(y, F(x; \theta, r))}{\partial z^{m,t}} \cdot \frac{\partial z^{m,t}}{\partial z^{m-1,t}} \\ &= g^{m,t} \cdot \frac{\partial z^{m,t}}{\partial z^{m-1,t}}. \end{aligned}$$

Performing gradient descent on  $r^m$  yields an update:

$$r^{m,t+1} \leftarrow (1 - \eta)r^{m,t} + \frac{\varepsilon}{k} \frac{g^{m,t}}{\|g^{m,t}\|_2}, \quad (2)$$

where  $\varepsilon$  is the stepsize and it is normalized by the number of steps  $k$ , so that the overall magnitude of update for  $k$  steps equals  $\varepsilon$ . The factor  $(1 - \eta)$  factor corresponds to the L2 regularization of the noise magnitude. Practically,  $\eta$  and  $\varepsilon$  control the contribution of the previous noise value  $r^{m,t}$  and the gradient  $g^{m,t}$  to the new noise  $r^{m,t+1}$ , respectively.

**Learning with a Noise Register** In practice, ANP is implemented efficiently in a backward-forward training process. Namely, for each mini-batch training we store the corresponding adversarial noise  $r$  for each hidden layer during backward propagation process; during forward propagation process, we simply fetch  $r$  as the noise and add to the input in the corresponding hidden layer after affine transformation and before activation function. This training procedure introduces no substantial increase in computation and memory consumption, except that we need to integrate a register  $S$  into each neuron for storing the adversarial noise  $r$  as

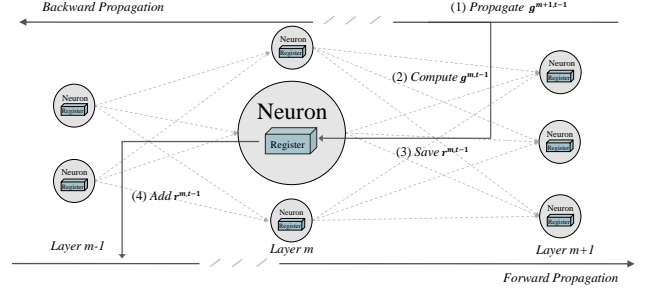


Figure 1: Adversarial noise propagation with the noise register during backward-forward training.

we illustrate in Figure 1. At the inference time,  $S$  can be discarded, leading to no influence on the model complexity. Algorithm 1 shows more details of the training process with ANP in each mini-batch.

---

### Algorithm 1 Adversarial Noise Propagation (ANP)

---

**Input:** mini-batch data  $(x, y)$

**Output:** robust model parameters  $\theta$

**Hyper-parameter:**  $\eta, \varepsilon$  and  $k$

---

- 1: **for**  $t$  in  $k$  steps **do**
  - 2:   // Backward propagation
  - 3:   Update model parameters  $\theta$  using standard back-propagation.
  - 4:   Compute and propagate adversarial gradient:  
 $g^{m,t-1} = g^{m+1,t-1} \cdot \frac{\partial z^{m+1,t-1}}{\partial z^{m,t-1}}$
  - 5:   Compute, propagate and save adversarial noise:  
 $r^{m,t} = (1 - \eta)r^{m,t-1} + \frac{\varepsilon}{k} \frac{g^{m,t-1}}{\|g^{m,t-1}\|_2}$
  - 6:   // Forward propagation
  - 7:   Compute the affine transformation:  
 $z^{m,t} = a^{m-1,t}w^{m-1} + b^{m-1}$
  - 8:   Fetch and add adversarial noise:  
 $z^{m,t} += r^{m,t}$
  - 9:   Compute the activation:  
 $a^{m,t} = \text{relu}(z^{m,t})$
  - 10: **end for**
- 

## Connections with the Related Works

ANP serves as a more general framework that observes adversarial noises in more flexible ways.

**Traditional adversarial training** The idea of traditional adversarial training stems from data augmentation. PGD-based adversarial training (PAT) (Madry et al. 2017) and new adversarial training (NAT) (Kurakin, Goodfellow, and Bengio 2016) train deep models with training data mixing clean examples as well as adversarial examples generated by PGD (Madry et al. 2017) and FGSM (Goodfellow, Shlens, and

Szegedy 2014), according to the following objective function:

$$\min_{\theta} \rho(\theta), \quad \rho(\theta) = \mathbb{E}_{(x,y) \sim D} \left[ \max_r L(y, F(x + r; \theta)) \right],$$

where  $r$  is a small ball that controls the magnitude of the noise. It is easy to see that both PAT and NAT only consider the adversarial noises in input data, which can be considered as a special case of ANP when we only consider adversarial noises in the 0-th hidden layer. Furthermore, the standard PAT and NAT typically only perform one step of gradient ascent on the adversarial noise, corresponding to the case of  $k = 1$  in our framework.

**Ensemble adversarial training (EAT)** To improve the diversity of adversarial examples, EAT (Tramèr et al. 2017) employs a set of models  $F$  to generate different adversarial examples for data augmentation. In ANP, various adversarial noises (with different noise sizes  $\varepsilon$ , iteration steps  $k$ , and noise magnitudes  $r$ ) are generated in each layer during training, increasing the diversity and complexity of adversarial noises injected into the model.

**Layer-wise adversarial training (LAT)** LAT (Sankaranarayanan et al. 2018) is proposed as a mechanism of regularization to prevent overfitting (and hence has the different goal from ANP). During their training time, adversarial gradients in current mini-batch are computed through the previous mini-batch. However, the adversarial noises in ANP for one specific mini-batch are computed only in the same mini-batch. We believe that the high correlation in one mini-batch will lead to better performance. Therefore, we introduce the progressive backward-forward propagation to fully utilize the information contained in every mini-batch data. Meanwhile, we take the contribution of previous noise during progressive iteration into consideration leading to better performance. Also, according to our study about the importance and effect of hidden layers in later section, only bottom layers should be considered during training to get robust model.

## Experiments and Evaluation

In this section, we will evaluate our proposed ANP in the popular image classification task. Following the guidelines from (Carlini et al. 2019), we compare ANP with the state-of-the-art adversarial defense methods against both adversarial noises and corruption as well.

### Experiments Settings

**Datasets and Models** For the adversarial robustness, we adopt the widely used **CIFAR-10** and **ImageNet** datasets. CIFAR-10 consists of 60K natural scene color images with 10 classes of size  $32 \times 32 \times 3$  (Krizhevsky and Hinton 2009). We use VGG-16, ResNet-18, DenseNet and InceptionV2 for CIFAR-10. ImageNet contains 14M images with more than 20k classes (Deng et al. 2009). For simplicity, we only choose 200 classes from 1000 in ILSVRC-2012 with 100K and 10k images for training set and test set, respectively. The models we use for ImageNet are ResNet-18

and AlexNet. We apply a diverse set of **adversarial attack models** including: FGSM (Goodfellow, Shlens, and Szegedy 2014), BIM (Kurakin, Goodfellow, and Bengio 2016), Step-LL (Kurakin, Goodfellow, and Bengio 2016), MI-FGSM (Dong et al. 2018), PGD (Madry et al. 2017), BPDA (Athalye, Carlini, and Wagner 2018) and C&W (Carlini and Wagner 2017). We also adopt MNIST, but show the experimental results in the supplementary materials due to the limited space.

For the corruption robustness, we test our proposed method on **CIFAR-10-C** and **CIFAR-10-P** (Hendrycks and Dietterich 2019). CIFAR-10-C and CIFAR-10-P are the first datasets for benchmarking model static and dynamic robustness against different common corruption and noise sequences under different severity levels (Hendrycks and Dietterich 2019). They are created from the test set of CIFAR-10 with 75 different corruption techniques, e.g., Gaussian noise, Poisson noise, Pixelation, etc.

As for comparative **defense models**, we choose the state-of-the-art defense methods including PAT (Madry et al. 2017), NAT (Kurakin, Goodfellow, and Bengio 2016), EAT (Tramèr et al. 2017), LAT (Sankaranarayanan et al. 2018) and Rand (Xie et al. 2018). Among these methods, EAT and Rand achieved No.1 in round 1 and No.2 in *NeurIPS 2017* adversarial defense competition.

In order to conduct fair experiments, we select the implementation and common hyper-parameters for attack and defense methods following their original papers and works, e.g., (Alexey, Ian, and Samy 2017; Carlini et al. 2019; Cisse et al. 2017; Madry et al. 2017), etc., which are comparable to other defense strategies.

### Evaluation Criteria

**Adversarial robustness** We use top-1 *worst case classification accuracy* in blackbox attack defense. For a specific test set, corresponding adversarial example sets are generated using attack methods from different hold-out models. Then, the final results are selected among them from the worst one. However, top-1 *classification accuracy* is utilized under whitebox attack. In this situation, adversaries know every details of target model and generate adversarial examples for direct attack.

**Corruption robustness** We adopt mCE, Relative mCE and mFR following (Hendrycks and Dietterich 2019). Among them, mCE denotes the mean corruption error with model compared to the baseline model, and Relative mCE represents the gap between mCE and the clean data error. Meanwhile, mFR stands for the classification differences between two adjacent frame in the noise sequence for a specific image. The formal definitions of these metrics are listed in the supplementary material.

### Is It Necessary to Inject Noises to All Layers?

Theoretical research on the representation power of neural network has been well studied (Hornik 1991; Delalleau and Bengio 2011). However, studies for hidden layers are rarely involved. Since every layer is not created equal (Zhang, Bengio, and Singer 2019), an intuitive question for ANP training

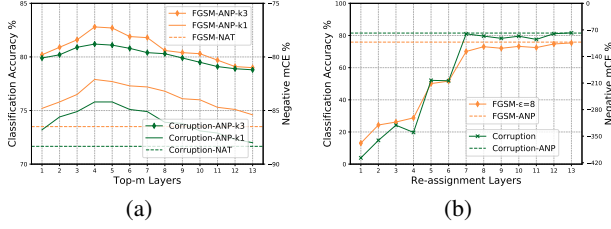


Figure 2: Subfigure(a) shows the results of VGG-16 trained with adversarial noises added to different layer groups. The solid lines denote models trained with different layer groups via ANP and the dashed lines represent baseline method NAT. Subfigure (b) denotes the layer weight re-assignment experiment where dashed lines show baseline model with no layer weight re-assignment, i.e., ANP.

emerged: *do we need to add noises to all layers?* In this section, we try to investigate the contribution of hidden layers when adversarial noises are injected and propagated.

We train a number of VGG-16 models on CIFAR-10 with adversarial noises injected into different layer groups namely, the top- $m$  layers. From the results in Figure 2 (a), we can observe that the model robustness ascends (i.e., both the classification accuracy for adversarial examples and the negative mCE for corruption increase) when injecting noises into the top- $m$  ( $m \leq 4$ ) hidden layers. Surprisingly, it is not true that the more layers injected with noises, more robust the model is. This indicates that different hidden layers contribute differently to model robustness in deep architecture. Bottom layers are more critical to model robustness while on the contrary the importance of upper layers is somewhat scarce. Thus, it is sufficient to *inject noises just into the bottom layers for better model robustness*, which will be used to guide our experiments in the rest of the paper.

Meanwhile, we trained ANP with the progressive number  $k=1$ , which is roughly similar to NAT with noises only confined to top-1 layer, as we discussed before. Its performance curves are shown by the orange and green solid lines without marker (ANP-k1) in Figure 2, which are almost close to that of NAT (1.5% difference due to implementation details), while much lower than the model trained with  $k=3$  (ANP-k3). This in turn proves the importance of our progressive noise injection for the model robustness.

We further investigate hidden layer contribution to robustness individually via layer weight re-assignment. Given a VGG-16 trained by ANP, we try to re-assign the layer weights of the model with a corresponding vanilla model at inference time. Analyzing each layer individually in the context of specific network architectures allows us to get more insights into the hidden layer behaviors. Intuitively, greater model performance gap after weight re-assignment means bigger weight differences, in turn indicating somewhat a more non-trivial hidden layer to model robustness. As shown in Figure 2 (b), the influence of individual layer weight re-assignment to model robustness reduces (classification accuracy for adversarial examples and negative mCE

for corruption arises) as the layer goes closer to the prediction. Thus, it double confirms that bottom layers are more critical to model robustness while on the contrary the importance of upper layers is somewhat scarce.

We also conduct the experiment for randomly perturbing each layer with gaussian noise  $N(0, 0.1)$ , see below for the brief results on CIFAR-10 with VGG-16, (clean, FGSM, mCE): 88.5%, 51.3%, 118.5%, which is worse than ANP. More experiments like ablation study and ANP on different model depths can be found in the supplementary material.

## Adversarial Robustness Evaluation

We first evaluate adversarial robustness for deep models through blackbox and whitebox attack defense.

**Blackbox attack defense** For blackbox attack defense, we train and compare each method with the same target model architecture over specific datasets. Adversarial example sets with 10k images are generated with various hold-out models different from the target models.

**CIFAR-10.** As shown in Table 6, on CIFAR-10 we employ VGG-16 as the target model and compare ANP with various defense methods. The hold-out models include ResNet-50, DenseNet and Inception-v2. Among defense methods, EAT is trained ensemble with VGG-16 and Inception-v2, meanwhile Rand resizes input images from 32 to 36 and follows a NAT trained VGG-16.

**ImageNet.** AlexNet is applied as the target model, and adversarial examples are generated from ResNet-18 and AlexNet. Meanwhile, EAT is trained with AlexNet and ResNet-18, and Rand resizes input images from 224 to 254 and follows a NAT trained AlexNet. The results on ImageNet are shown in Table 10.

From the above blackbox experiments, we obtain the following observations: (1) Under blackbox setting, in almost all cases ANP achieves the best defense performance among all methods. (2) ANP enables strong robustness to the widely-used deep models against both single-step and iterative blackbox attacks. (3) Usually the classification performance to clean examples degrades fiercely when introducing more noise in the model, e.g., 5% to 10% accuracy decrease. However, ANP supplies the models with good generalization ability, keeping the stable and close classification accuracy to the Vanilla models on CIFAR-10 as well as MNIST. Due to the limited space, more experimental results can be found in the supplementary material.

**Whitebox attack defense** In whitebox scenario, we apply PGD, C&W and the attacking framework BPDA for their strong attack abilities. Moreover, BIM is utilized in BPDA to demonstrate whitebox attack after circumventing the gradient mask with iterative number 5. The results on CIFAR-10 and ImageNet are listed in Table 8.

From these tables, we can conclude that under whitebox setting ANP owns significant advantages on defending against adversarial examples over other methods on these datasets, though slightly weak performance of ANP on PGD attack under ImageNet is witnessed compared to PAT. The overall results indicate that ANP with diversified noises enables model robustness against various attack methods and

Table 1: Blackbox attack defense results on CIFAR-10 with VGG-16.

VGG-16	CLEAN	FGSM		PGD		STEP-LL	MI-FGSM
		$\epsilon = 8$	$\epsilon = 16$	$\epsilon = 8, \alpha = 16$	$\epsilon = 8, \alpha = 2$	$\epsilon = 8$	$\epsilon = 8$
VANILLA	<b>92.1%</b>	38.4%	19.3%	9.7%	0.0%	7.5%	2.3%
PAT	85.1%	82.3%	<b>76.4%</b>	84.2%	82.1%	80.1%	77.5%
NAT	86.1%	73.5%	70.2%	82.1%	80.3%	79.1%	72.6%
LAT	84.4%	75.8%	63.7%	83.2%	79.2%	78.3%	71.4%
RAND	85.2%	77.6%	70.8%	82.5%	80.2%	79.3%	73.2%
EAT	87.5%	81.2%	76.2%	85.1%	83.5%	82.7%	75.8%
ANP	91.7%	<b>82.8%</b>	<b>76.4%</b>	<b>86.9%</b>	<b>84.4%</b>	<b>83.3%</b>	<b>80.1%</b>

Table 2: Blackbox attack defense results on ImageNet with AlexNet.

ALEXNET	CLEAN	FGSM		PGD		STEP-LL	MI-FGSM
		$\epsilon = 8$	$\epsilon = 16$	$\epsilon = 8, \alpha = 16$	$\epsilon = 8, \alpha = 2$	$\epsilon = 8$	$\epsilon = 8$
VANILLA	<b>61.7%</b>	12.6%	9.2%	4.2%	4.3%	13.7%	3.5%
PAT	55.2%	41.5%	<b>40.2%</b>	41.9%	<b>42.1%</b>	41.5%	<b>40.3%</b>
NAT	53.3%	39.1%	34.2%	39.5%	39.6%	41.6%	34.7%
RAND	50.2%	39.2%	27.0%	40.1%	39.2%	40.9%	33.5%
EAT	55.0%	39.6%	35.2%	40.0%	39.9%	42.3%	36.8%
ANP	53.5%	<b>41.7%</b>	39.3%	<b>42.0%</b>	<b>42.1%</b>	<b>42.7%</b>	<b>40.3%</b>

enjoys strong capability of covering the varying decision space in practice. However, we also witnessed that for big dataset like ImageNet, clean accuracy drops for all methods. The reasons might be two-folded. Firstly, adversarial robust models need bigger capacity (Tsipras et al. 2018). However, Alexnet, a relatively small model, may not have enough capacity to fit adversarial noises while keeping high accuracy on clean examples. Secondly, trade-off between robustness and accuracy does exist (Zhang et al. 2019) especially for high-dimensional data. We will study it in the future.

### Corruption Robustness Evaluation

For corruption robustness, we conduct the experiment with 10K images from CIFAR-10-C with 15 different corruption and 5 severity levels. To test model dynamic robustness, we use CIFAR-10-P which differs from CIFAR-10-C with noise sequences generated for each image with more than 30 frames. As shown in the supplementary material, mCE indicates the average corruption error and mFR is the average flip rate of noise sequence showing the model resistance to noise sequence (both the lower the better). According to the results in Figure 3 (a) and (b), ANP achieves the lowest mCE and mFR value among all methods indicating strong corruption robustness. More precisely, as shown in Table 4, ANP surpasses comparative strategies with big margins, i.e., almost 6 and 30 for mCE and mFR, respectively. The results mean that ANP can faithfully bring both static and dynamic robustness against corruption.

Comparative methods, especially PAT, though perform good on adversarial examples, show weak robustness to corruption. Also, an interesting phenomenon can be observed that all comparative strategies even perform worse than

Table 3: Whitebox attack defense on CIFAR-10 and ImageNet.

(a) CIFAR-10 with VGG-16				
VGG-16	CLEAN	BPDA	PGD	C&W
		$\epsilon=8$	$\epsilon=8$	$c=0.2$
VANILLA	<b>92.1%</b>	0.2%	0.0%	8.2%
PAT	85.1%	40.5%	27.6%	41.4%
NAT	86.1%	24.5%	8.1%	31.6%
RAND	85.2%	0.2%	9.1%	34.2%
EAT	87.5%	37.6%	9.9%	35.2%
ANP	91.7%	<b>43.5%</b>	<b>27.9%</b>	<b>48.1%</b>

(b) ImageNet with AlexNet			
ALEXNET	CLEAN	BPDA	PGD
		$\epsilon=8$	$\epsilon=8$
VANILLA	<b>61.7%</b>	7.9%	2.4%
PAT	55.2%	27.6%	<b>28.7%</b>
NAT	53.3%	26.8%	15.2%
RAND	50.2%	21.6%	16.7%
EAT	55.0%	25.0%	12.5%
ANP	53.5%	<b>28.2%</b>	27.4%

Vanilla model for dynamic corruption (showing in higher mFR values). Most adversarial training methods attempt to inject noises to inputs by searching for the worst-case perturbations which indeed improve adversarial model robustness. However, their tactics seem to be worthless to average-case perturbations, or even counteractive to corruption robustness. Since robustness requires high data complexity



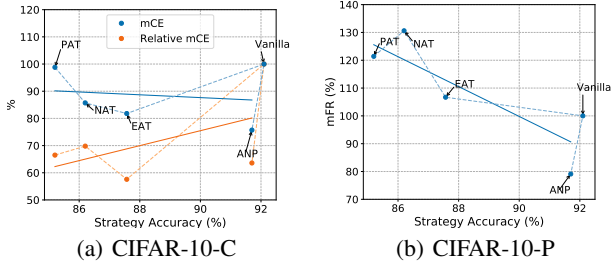


Figure 3: Model corruption robustness evaluation.

Table 4: Corruption robustness evaluation with mCE and mFR.

VGG-16	ERROR	MCE	MFR
VANILLA	<b>7.9</b>	100.0	100.0
PAT	14.9	98.6	122.9
NAT	13.9	85.7	131.2
EAT	12.5	81.8	108.3
<b>ANP</b>	<b>8.3</b>	<b>75.7</b>	<b>79.2</b>

(Schmidt et al. 2018), our ANP introduces noises with high complexity and diversity via progressive iteration contributing both adversarial and corruption robustness. Thus, we can draw the conclusion that ANP builds robust model against corruption compared to other defense methods.

### What Did Hidden Layers Do during Noise Propagation?

In this section, we try to uncover the behaviors and effects of hidden layers during noise propagation from views of hidden representation insensitivity and human vision alignment.

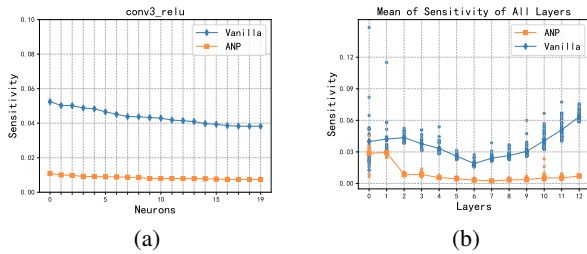


Figure 4: Hidden representation insensitivity on relu of conv3 layer and mean for all layers.

At a high-level perspective, robustness to noises can be viewed as a global insensitivity property that a model satisfies (Tsipras et al. 2018). A model that achieves small loss for noises in a dataset, will necessarily learn representations that are insensitive to such noises. By injecting adversarial noises to hidden layers, ANP can be viewed as a method to embed certain insensitivity in each hidden representation for models. Thus, we try to explain hidden layer behaviors from

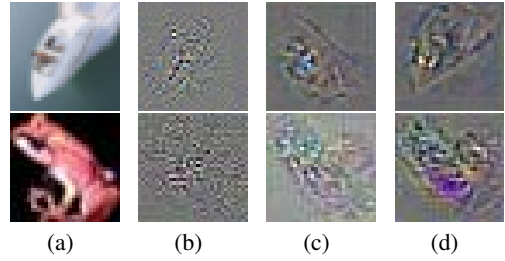


Figure 5: Visualization of the loss gradient w.r.t. input pixels on CIFAR-10. Subfigure (a) denotes the input image, (b) to (d) represent gradients gained from Vanilla model, ANP on top-all layers and ANP on top-4 layers, respectively.

the view of hidden representation insensitivity. We measure the hidden representation insensitivity based on the change degree of neuron activation value within pairs of sample  $(x, x')$  in which the distance between each pair is constrained with  $\epsilon$ . Intuitively, when fed with benign and polluted examples, more insensitively neurons behave, more robust the models are. As shown in Figure 4, neurons in each layer behave more insensitively to  $\epsilon$ -noises (PGD attack adversarial examples and corruption) after trained with ANP.

Lastly, we explain model robustness from the view of alignment with human vision perception that stronger model gains more semantically meaningful gradient. As shown in Figure 10, we observe that gradients for ANP trained networks on top-4 layers (d) align well with perceptual features (such as edges) of input images. On the contrary, these gradients have no coherent patterns and appear very noisy to humans for Vanilla networks (b), and are less semantically meaningful for ANP trained model on all layers (c).

## Conclusion

In order to improve model robustness against noises, this paper proposes a training strategy named *Adversarial Noise Propagation* (ANP), which injects diversified noises into the hidden layers in a layer-wise way. Also, ANP can be implemented efficiently through standard backward-forward process hence introducing no additional computations. Extensive experiments on the visual classification task demonstrate that ANP can enable the strong robustness for deep networks, and thus help obtain very promising performance against various types of noises. For future work, we are interested in devising a more adaptive algorithm which considers the heterogeneous behaviors of different layers.

## References

- [Alexey, Ian, and Samy 2017] Alexey, K.; Ian, G.; and Samy, B. 2017. Adversarial machine learning at scale. In *International Conference on Learning Representations*.
- [Athalye, Carlini, and Wagner 2018] Athalye, A.; Carlini, N.; and Wagner, D. 2018. Obfuscated gradients give a false sense of security: Circumventing defenses to adversarial examples. *arXiv preprint arXiv:1802.00420*.

- [Bahdanau, Cho, and Bengio 2014] Bahdanau, D.; Cho, K.; and Bengio, Y. 2014. Neural machine translation by jointly learning to align and translate. *arXiv preprint arXiv:1409.0473*.
- [Carlini and Wagner 2017] Carlini, N., and Wagner, D. 2017. Towards evaluating the robustness of neural networks. In *2017 IEEE Symposium on Security and Privacy (SP)*, 39–57. IEEE.
- [Carlini et al. 2019] Carlini, N.; Athalye, A.; Papernot, N.; Brendel, W.; Rauber, J.; Tsipras, D.; Goodfellow, I.; and Madry, A. 2019. On evaluating adversarial robustness. *arXiv preprint arXiv:1902.06705*.
- [Cisse et al. 2017] Cisse, M.; Bojanowski, P.; Grave, E.; Dauphin, Y.; and Usunier, N. 2017. Parseval networks: Improving robustness to adversarial examples. In *International Conference on Machine Learning*.
- [Cortes and Vapnik 1995] Cortes, C., and Vapnik, V. 1995. Support-vector networks. *Machine learning* 20(3):273–297.
- [Delalleau and Bengio 2011] Delalleau, O., and Bengio, Y. 2011. Shallow vs. deep sum-product networks. In *Advances in Neural Information Processing Systems*, 666–674.
- [Deng et al. 2009] Deng, J.; Dong, W.; Socher, R.; Li, L.-J.; Li, K.; and Fei-Fei, L. 2009. Imagenet: A large-scale hierarchical image database. In *IEEE Conference on Computer Vision and Pattern Recognition*.
- [Dhillon et al. 2018] Dhillon, G. S.; Azizzadenesheli, K.; Lipton, Z. C.; Bernstein, J.; Kossaifi, J.; Khanna, A.; and Anandkumar, A. 2018. Stochastic activation pruning for robust adversarial defense. In *International Conference on Learning Representations*.
- [Dodge and Karam 2017] Dodge, S., and Karam, L. 2017. A study and comparison of human and deep learning recognition performance under visual distortions. In *International Conference on Computer Communication and Networks*.
- [Dong et al. 2018] Dong, Y.; Liao, F.; Pang, T.; and Su, H. 2018. Boosting adversarial attacks with momentum. In *IEEE Conference on Computer Vision and Pattern Recognition*.
- [Elsayed et al. 2018] Elsayed, G.; Krishnan, D.; Mobahi, H.; Regan, K.; and Bengio, S. 2018. Large margin deep networks for classification. In *Advances in Neural Information Processing Systems 31*. 850–860.
- [Goodfellow, Shlens, and Szegedy 2014] Goodfellow, I. J.; Shlens, J.; and Szegedy, C. 2014. Explaining and harnessing adversarial examples (2014). *arXiv preprint arXiv:1412.6572*.
- [He, Li, and Song 2018] He, W.; Li, B.; and Song, D. 2018. Decision boundary analysis of adversarial examples. In *International Conference on Learning Representations*.
- [Hendrycks and Dietterich 2019] Hendrycks, D., and Dietterich, T. 2019. Benchmarking neural network robustness to common corruptions and perturbations. In *International Conference on Learning Representations*.
- [Hinton et al. 2012] Hinton, G.; Deng, L.; Yu, D.; Dahl, G. E.; Mohamed, A.; Jaitly, N.; Senior, A.; Vanhoucke, V.; Nguyen, P.; and Sainath, T. N. 2012. Deep neural networks for acoustic modeling in speech recognition: The shared views of four research groups. *IEEE Signal Processing Magazine* 29(6):82–97.
- [Hornik 1991] Hornik, K. 1991. Approximation capabilities of multilayer feedforward networks. *Neural networks* 4(2):251–257.
- [Ilyas et al. 2019] Ilyas, A.; Santurkar, S.; Tsipras, D.; Engstrom, L.; Tran, B.; and Madry, A. 2019. Adversarial examples are not bugs, they are features. *arXiv preprint arXiv:1905.02175*.
- [Krizhevsky and Hinton 2009] Krizhevsky, A., and Hinton, G. 2009. Learning multiple layers of features from tiny images. Technical report, Citeseer.
- [Krizhevsky, Sutskever, and Hinton 2012] Krizhevsky, A.; Sutskever, I.; and Hinton, G. E. 2012. Imagenet classification with deep convolutional neural networks. In *International Conference on Neural Information Processing Systems*, 1097–1105.
- [Kurakin, Goodfellow, and Bengio 2016] Kurakin, A.; Goodfellow, I.; and Bengio, S. 2016. Adversarial examples in the physical world. *arXiv preprint arXiv:1607.02533*.
- [Liao et al. 2018] Liao, F.; Liang, M.; Dong, Y.; Pang, T.; Hu, X.; and Zhu, J. 2018. Defense against adversarial attacks using high-level representation guided denoiser. In *IEEE Conference on Computer Vision and Pattern Recognition*.
- [Liu et al. 2019] Liu, A.; Liu, X.; Fan, J.; Ma, Y.; Zhang, A.; Xie, H.; and Tao, D. 2019. Perceptual-sensitive gan for generating adversarial patches. In *33rd AAAI Conference on Artificial Intelligence*.
- [Madry et al. 2017] Madry, A.; Makelov, A.; Schmidt, L.; Tsipras, D.; and Vladu, A. 2017. Towards deep learning models resistant to adversarial attacks. *arXiv preprint arXiv:1706.06083*.
- [Papernot et al. 2016] Papernot, N.; McDaniel, P.; Goodfellow, I.; Jha, S.; Celik, Z. B.; and Swami, A. 2016. Practical black-box attacks against deep learning systems using adversarial examples. *arXiv preprint*.
- [Sankaranarayanan et al. 2018] Sankaranarayanan, S.; Jain, A.; Chellappa, R.; and Lim, S. N. 2018. Regularizing deep networks using efficient layerwise adversarial training. In *32nd AAAI Conference on Artificial Intelligence*.
- [Santurkar et al. 2019] Santurkar, S.; Tsipras, D.; Tran, B.; Ilyas, A.; Engstrom, L.; and Madry, A. 2019. Computer vision with a single (robust) classifier. *arXiv preprint arXiv:1906.09453*.
- [Schmidt et al. 2018] Schmidt, L.; Santurkar, S.; Tsipras, D.; Talwar, K.; and Madry, A. 2018. Adversarially robust generalization requires more data. In *Advances in Neural Information Processing Systems*, 5014–5026.
- [Szegedy et al. 2013] Szegedy, C.; Zaremba, W.; Sutskever, I.; Bruna, J.; Erhan, D.; Goodfellow, I.; and Fergus, R. 2013. Intriguing properties of neural networks. *arXiv preprint arXiv:1312.6199*.
- [Tramèr et al. 2017] Tramèr, F.; Kurakin, A.; Papernot, N.; Goodfellow, I.; Boneh, D.; and McDaniel, P. 2017. En-



semble adversarial training: Attacks and defenses. *arXiv preprint arXiv:1705.07204*.

[Tsipras et al. 2018] Tsipras, D.; Santurkar, S.; Engstrom, L.; Turner, A.; and Madry, A. 2018. Robustness may be at odds with accuracy. *stat* 1050:11.

[Xie et al. 2018] Xie, C.; Wang, J.; Zhang, Z.; Ren, Z.; and Yuille, A. 2018. Mitigating adversarial effects through randomization. In *International Conference on Learning Representations*.

[Xu and Mannor 2012] Xu, H., and Mannor, S. 2012. Robustness and generalization. *Machine learning* 86(3):391–423.

[Yan, Guo, and Zhang 2018] Yan, Z.; Guo, Y.; and Zhang, C. 2018. Deep defense: Training dnns with improved adversarial robustness. In *Advances in Neural Information Processing Systems 31*. 417–426.

[Zhang, Bengio, and Singer 2019] Zhang, C.; Bengio, S.; and Singer, Y. 2019. Are all layers created equal? *arXiv preprint arXiv:1902.01996*.

[Zhang et al. 2019] Zhang, H.; Yu, Y.; Jiao, J.; Xing, E. P.; Ghaoui, L. E.; and Jordan, M. I. 2019. Theoretically principled trade-off between robustness and accuracy. *arXiv preprint arXiv:1901.08573*.

[Zheng et al. 2016] Zheng, S.; Song, Y.; Leung, T.; and Goodfellow, I. 2016. Improving the robustness of deep neural networks via stability training. In *IEEE conference on computer vision and pattern recognition*.

## Appendix

### Adversarial Attack Algorithms

Finding an adversarial example is equivalent to solve the non-convex optimization problem, which is hard to calculate directly. Thus, many adversarial attack methods have been proposed to solve the problem. Here, a brief introduction of the most widely used ones is shown below:

**Fast Gradient Sign Method (FGSM).** Goodfellow, Shlens, and Szegedy proposes FGSM as a simple way to generate adversarial examples. This method is simple and computationally efficient compared to more complex methods like L-BFGS:

$$x^{adv} = x + \epsilon \cdot \text{sign}(\nabla_x J(x, y_{true})).$$

**Basic Iterative Method (BIM).** A straightforward extension of FGSM is BIM (Kurakin, Goodfellow, and Bengio 2016) which applies it multiple times with small step size:

$$\begin{aligned} x_0^{adv} &= x, \\ x_{n+1}^{adv} &= \text{Clip}_{x, \epsilon} \{x_n^{adv} + \alpha \cdot \text{sign}(\nabla_x J(x_n^{adv}, y_{true}))\}. \end{aligned}$$

**Single-Step Least-Likely Class Method (Step-LL).** This variant of FGSM introduced by Kurakin, Goodfellow, and Bengio targets the least-likely class,  $y_{LL} = \text{argmin}_f(x)$ :

$$x^{adv} = x - \epsilon \cdot \text{sign}(\nabla_x J(F(x), y_{LL})).$$

**Momentum Iterative FGSM (MI-FGSM).** As an iterative gradient-based attack method, MI-FGSM (Dong et al. 2018) utilizes momentum to boost attack performance achieving No.1 in *NIPS 2017* adversarial attack competition:

$$\begin{aligned} g_{n+1} &= \mu \cdot g_n + \frac{\nabla_x J(x_n^{adv}, y_{true})}{\|\nabla_x J(x_n^{adv}, y_{true})\|_1}, \\ x_{n+1}^{adv} &= x_n^{adv} + \alpha \cdot \text{sign}(g_{n+1}). \end{aligned}$$

**Projected Gradient Descent (PGD).** A more powerful adversary is the iterative variant of FGSM, which is essentially projected gradient descent on the negative loss function (Madry et al. 2017):

$$\begin{aligned} x_0^{adv} &= x, \\ x_{n+1}^{adv} &= \Pi_{x, S} \{x_n^{adv} + \alpha \cdot \text{sign}(\nabla_x J(x_n^{adv}, y_{true}))\}. \end{aligned}$$

**Backward Pass Differentiable Approximation (BPDA).** Athalye, Carlini, and Wagner proposes an adversarial attack framework which circumvents the non-differentiable input filter by conducting iterative gradient-based whitebox attack on  $x$  directly. BPDA successfully breaks 7 of 9 adversarial defense strategies in *ICLR 2018*.

**Carlini & Wagner (C&W).** Given  $x$ , C&W  $L_2$  attack Carlini and Wagner searches for  $w$  with a target class  $t$  that solves:

$$\min \left\| \frac{1}{2}(\tanh(w) + 1) - x \right\|_2^2 + c \cdot f\left(\frac{1}{2}(\tanh(w) + 1)\right),$$

with  $F$  defined as:

$$F(x') = \max(\max\{Z(x')_i : i \neq t\} - Z(x')_t, k).$$

### Definition of Model Corruption Robustness Evaluation Criteria

In order to comprehensively evaluate a classifier’s robustness to corruption, Hendrycks and Dietterich proposed three different metrics to score the performance of a classifier.

**mCE.** The first evaluation step is to take a trained classifier  $f$ , which has not been trained on CIFAR10-C, and compute the clean dataset top-1 error rate as  $E_{clean}^F$ . The second step is to test the classifier on each corruption type  $c$  at each level of severity  $s$  denoted as  $E_{s,c}^F$ . They adjust for the varying difficulties by dividing by errors of a baseline model. Finally, mCE is computed as follows:

$$CE_c^F = \frac{\sum_{s=1}^5 E_{s,c}^F}{\sum_{s=1}^5 E_{s,c}^{base}}.$$

Thus, mCE is the average of 15 different Corruption Errors (CE).

**Relative mCE.** A more nuanced corruption robustness measure is Relative mCE. If a classifier withstands most corruption, the gap between mCE and the clean data error is minuscule. So, Relative mCE is calculated as follows:

$$\text{Relative mCE}_c^F = \frac{\sum_{s=1}^5 E_{s,c}^F - E_{clean}^F}{\sum_{s=1}^5 E_{s,c}^{base} - E_{clean}^{base}},$$

whereas Relative mCE is the average score of them.

**mFR.** Let us denote  $m$  noise sequences with  $S = \{(x_1^{(i)}, x_2^{(i)}, \dots, x_n^{(i)})\}_{i=1}^m$  where each sequence is made with noise  $p$ . The ‘Flip Probability’ of network  $F: x \rightarrow \{1, 2, 3, \dots, 1000\}$  on noise sequences  $S$  is:

$$FP_p^F = \frac{1}{m(n-1)} \sum_{i=1}^m \sum_{j=2}^n 1(F(x_j^{(i)}) \neq F(x_{j-1}^{(i)})) \\ = \mathbb{P}_{x \sim S}((F(x_j) \neq F(x_{j-1}))).$$

Then, the Flip Rate  $FR_p^F = FP_p^F / FP_p^{base}$  and mFR is the average value of FR.

## Overall Training Phases

In order to make the model robust against various types of real-world noises, and simultaneously achieve a strong generalization ability on clean examples, we need to carefully control the magnitude of the noise to balance overfitting and underfitting. To achieve this, we propose to divide our training procedure into three phases, each fed with adversarial noise with different magnitude:

**Phase 1: Zero Adversarial Noise (Clean Examples).** This phase utilizes only clean examples in order to achieve a good starting point of our deep neural networks. Without any noises, we can quickly train a model to have a basic classification ability, avoiding instability before we find a reasonably good model.

**Phase 2: Large Adversarial Step Size.** In this phase, we introduce adversarial noise by using a relatively large adversarial step size  $\epsilon$  to further train deep learning models. This allows us to quickly improve noise resistance ability of the models, and strongly push the decision boundary away from the data points to increase robustness against adversarial examples. Meanwhile, using large step size allows us to run smaller number  $k$  of gradient steps, and hence saves computation.

**Phase 3: Small Adversarial Step Size.** Large adversarial step size increases the robustness, but may hurt the prediction performance. In the final phase, we decrease the adversarial step size so that the model is properly fine tuned to achieve a better balance between robustness and prediction accuracy.

## More Experiment Results

### Top-m Layer Group Noise Study

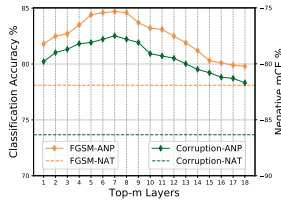


Figure 6: Top-m layer group noise study with ResNet-18.

In this section, we show the results of models trained with adversarial noises added to different layer groups using ResNet-18. The solid lines denote models trained with different layer groups via ANP and the dashed lines represent baseline

method NAT. From the results in Figure 6, we can observe that the model robustness ascends as both the classification accuracy for adversarial examples and the negative mCE for corruption increase when adversarial noises are injected into the top- $m$  ( $m \leq 7$ ) hidden layers. The experimental results also confirm our above conclusion that *Bottom layers are more critical to model robustness while on the contrary the importance of upper layers is somewhat scarce* on different deep architectures.

## Adversarial Robustness Evaluation

**CIFAR-10.** The results of blackbox and whitebox attack defense on CIFAR-10 with ResNet-18 are listed in Table 5 and 6. As we can see, ANP outperforms other defensive strategies on both blackbox and whitebox scenarios.

**MNIST.** With LeNet as the target model, the experimental results of blackbox and whitebox are listed in Table 7.

Table 5: Whitebox attack defense results on CIFAR-10 with ResNet-18.

RESNET-18	CLEAN	BPDA	PGD	C&W
		$\epsilon=8$	$\epsilon=8$	$c=0.2$
VANILLA	<b>93.1%</b>	0.0%	2.7%	8.4%
PAT	85.6%	45.2%	28.9%	43.7%
NAT	89.1%	33.5%	10.1%	32.6%
RAND	86.4%	1.9%	9.4%	31.2%
EAT	86.9%	40.1%	14.5%	39.1%
<b>ANP</b>	92.1%	<b>54.0%</b>	<b>29.0%</b>	<b>47.3%</b>

## Corruption Robustness Evaluation

Corruption robustness experiment results are presented in Table 8, 9 and 10. As for mCE and mFR, ANP outperforms other methods greatly with the lowest values showing the strong corruption robustness. However, the value of Relative mCE for ANP is slightly higher than EAT, ranking the second place. The reason is that the error rate of ANP for clean examples is much lower than that of EAT and the larger subtrahend of numerator in the formula contributes to a smaller result of EAT model. We also test a VGG-16 model trained with Gaussian noise  $N(0, 0.1)$  added to input, but the results turn to be weak to corruption with a mCE value 117.2.

## Model Robustness Evaluation with Proposed Criteria

Standard methods (Alexey, Ian, and Samy 2017; Athalye, Carlini, and Wagner 2018), usually evaluate model robustness only depending on classification accuracy which reveals limited information regarding how and why robustness is achieved. To further understand how ANP behaves in improving the model robustness, we investigate the performance of different methods via our proposed criteria *Worst Case Boundary Distance* and  $\epsilon$  - *Empirical Noise Insensitivity* based on decision boundary distance and Lipschitz constant.

Table 6: Blackbox attack defense results on CIFAR-10 with ResNet-18.

RESNET-18	CLEAN	FGSM		PGD		STEP-LL	MI-FGSM
		$\epsilon = 8$	$\epsilon = 16$	$\epsilon = 8, \alpha = 16$	$\epsilon = 8, \alpha = 2$	$\epsilon = 8$	$\epsilon = 8$
VANILLA	<b>93.1%</b>	12.8%	10.2%	6.3%	6.0%	21.4%	1.0%
PAT	85.6%	81.5%	72.1%	<b>85.5%</b>	84.9%	81.2%	76.7%
NAT	89.1%	78.1%	68.8%	80.8%	83.6%	80.4%	73.2%
LAT	88.9%	72.8%	69.1%	69.3%	68.3%	72.3%	70.8%
RAND	86.4%	77.6%	68.0%	75.7%	72.4%	71.0%	69.0%
EAT	86.9%	80.8%	72.5%	83.7%	84.7%	82.8%	80.0%
<b>ANP</b>	92.1%	<b>83.6%</b>	<b>73.5%</b>	<b>85.5%</b>	<b>86.5%</b>	<b>84.0%</b>	<b>80.1%</b>

Table 7: Blackbox and whitebox attack defense results on MNIST with LeNet.

LENET	CLEAN	BLACKBOX			WHITEBOX		
		FGSM			BPDA	PGD	C&W
		$\epsilon=0.1$	$\epsilon=0.2$	$\epsilon=0.3$	$\epsilon=0.2$	$\epsilon=0.2$	$c=0.2$
VANILLA	<b>99.6%</b>	72.0%	28.0%	4.0%	61.7%	22.3%	27.1%
PAT	99.0%	96.8%	90.7%	<b>78.0%</b>	90.6%	<b>59.1%</b>	63.7%
NAT	98.4%	94.0%	88.0%	72.0%	85.9%	45.1%	51.4%
<b>ANP</b>	99.3%	<b>97.1%</b>	<b>93.2%</b>	<b>78.0%</b>	<b>91.5%</b>	<b>59.1%</b>	<b>69.1%</b>

Table 8: Corruption Error and mCE values of different corruption and strategies on CIFAR-10-C. The mCE value is the mean Corruption Error of the corruption in Noise, Blur, Weather, and Digital columns. All models are not trained on CIFAR-10-C images.

Network	Error	MCE	Noise				Blur				Weather					Digital			
			Gaussian	Shot	Impulse	Speckle	Defocus	Glass	Motion	Zoom	Gaussian	Spatter	Snow	Frost	Fog	Bright	Contrast	Elastic	Pixel
VANILLA	<b>7.9</b>	100.0	100	100	100	100	100	100	100	100	100	100	100	100	100	100	100	100	
PAT	14.9	98.6	41	47	59	52	90	43	89	84	72	95	97	94	208	206	154	110	62
NAT	13.9	85.7	51	58	105	63	89	52	90	81	83	91	80	65	136	111	112	102	67
EAT	12.5	81.8	37	44	50	47	84	46	94	75	74	87	77	70	152	125	126	102	63
<b>ANP</b>	8.3	<b>75.7</b>	36	41	59	45	82	51	85	76	77	79	70	61	140	99	123	90	55

Table 9: Relative Corruption Errors and Relative mCE values of different corruption and strategies on CIFAR-10-C. All models are not trained on CIFAR-10-C images.

NETWORK	ERROR	REL.MCE	NOISE				BLUR				WEATHER				DIGITAL			
			GAUSSIAN	SHOT	IMPULSE	SPECKLE	DEFOCUS	GLASS	MOTION	ZOOM	GAUSSIAN	SPATTER	SNOW	FROST	FOG	BRIGHT	CONTRAST	ELASTIC
VANILLA	<b>7.9</b>	100	100	100	100	100	100	100	100	100	100	100	100	100	100	100	100	100
PAT	14.9	68.1	11	15	33	18	65	43	75	54	60	65	55	51	183	162	140	81
NAT	13.9	69.8	35	38	102	44	69	36	76	61	67	69	57	39	157	99	111	89
EAT	12.5	<b>57.6</b>	14	15	28	17	49	24	75	44	47	49	44	40	175	122	126	76
<b>ANP</b>	8.3	<b>63.6</b>	20	21	47	25	66	38	77	61	64	58	50	41	175	98	131	80

**Worst Case Boundary Distance** The minimum distance to the decision boundary among data points reflects the model robustness to small noises (Cortes and Vapnik 1995; Elsayed et al. 2018). Due to the computation difficulty for decision boundary distance, we propose *Worst Case Boundary Distance* (denoted as  $W_f$ ) in a heuristic way. A larger  $W_f$  means a stronger model. Given a learnt model  $f$  and point  $x_i$  with class label  $y_i$  ( $i = 1, \dots, N$ ), we first generate a set  $V$  of  $m$  random orthogonal directions (He, Li, and Song 2018). Then, for each direction in  $V$  we estimate

the root mean square (RMS) distances  $\phi_i(V)$  to the decision boundary of  $f$ , until the model’s prediction changes, i.e.,  $f(x_i) \neq y_i$ . Among  $\phi_i(V)$ ,  $d_i$  denotes the minimum distance (i.e., the worst case) moved to change the prediction for instance  $x_i$ . Then our *Worst Case Boundary Distance* is defined as follows:

$$W_f = \frac{1}{N} \sum_{i=1}^N d_i, \quad d_i = \min \phi_i(V). \quad (3)$$

We choose 1,000 randomly selected orthogonal direc-

Table 10: Flip Rates and the mFR values of different perturbations and strategies on CIFAR-10-P. All models are not trained on CIFAR-10-P images.

NETWORK	ERROR	mFR	NOISE			BLUR			WEATHER			DIGITAL		
			GAUSSIAN	SHOT	SPECKLE	MOTION	ZOOM	GAUSSIAN	BRIGHT	SPATTER	SNOW	TRANSLATE	ROTATE	TILT
VANILLA	<b>7.9</b>	100	100	100	100	100	100	100	100	100	100	100	100	100
PAT	14.9	122.9	106	100	99	103	185	173	137	119	116	110	104	129
NAT	13.9	131.2	119	114	114	107	249	219	140	117	97	110	97	137
EAT	12.5	108.3	107	104	105	99	119	120	123	118	99	107	91	108
<b>ANP</b>	<b>8.3</b>	<b>79.2</b>	82	84	85	86	73	76	86	87	76	79	70	76

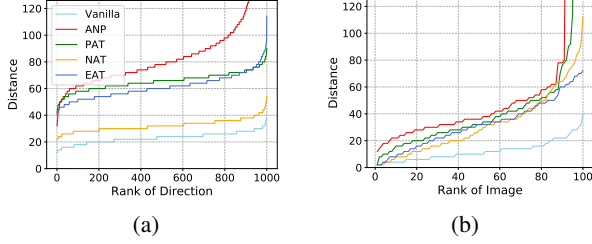


Figure 7: Worst Case Boundary Distance are computed among five different VGG-16 models to change the predicted label: (a) the average distance moved in each orthogonal direction, and (b) the minimum distance (i.e., Worst Case Boundary Distance) moved for 100 different images.

tions, and compute the minimum distance along each direction for a specific image to change the predicted label. As shown in Figure 7 (a), models trained by ANP own the largest distance. Meanwhile, Figure 7 (b) gives the minimum distances moved for each of 100 randomly picked images to change their labels. It is easy to see that the distance curve of ANP maintains almost the highest, with a big leading gap at the beginning. Table 11 further reports  $W_f$  for different methods. The results consistently prove that ANP enables the learnt deep models to have the strong discriminating power with the large margins, thus obtain the most robust model.

Table 11: Worst Case Boundary Distance among five VGG-16 models trained with different training methods.

METHOD	VANILLA	PAT	NAT	EAT	ANP
$W_f$	29.46	41.05	34.22	35.21	<b>47.36</b>

**$\epsilon$ -Empirical Noise Insensitivity** Xu and Mannor first introduced the concept of learning algorithms robustness from the idea that if two samples are “similar” then their test errors are very close. Inspired by that, we propose  *$\epsilon$ -Empirical Noise Insensitivity* to measure model robustness against generalized noise from the view of Lipschitz constant, and a lower value indicates a stronger model. We first select  $N$  clean examples randomly, then  $M$  examples are generated

from each clean example via various methods, e.g., adversarial attack, Gaussian noise, blur, etc. The differences between model loss function are computed when clean example and corresponding polluted examples are fed to. The different severities in loss function is used to measure model insensitivity and stability to generalized small noises within constraint  $\epsilon$ :

$$I_f(\epsilon) = \frac{1}{N \times M} \sum_{i=1}^N \sum_{j=1}^M \frac{|l_f(x_i|y_i) - l_f(\mu_{ij}|y_i)|}{|x_i - \mu_{ij}|_\infty} \quad (4)$$

$$s.t. \quad |x_i - \mu_{ij}|_\infty \leq \epsilon,$$

where  $x_i$ ,  $\mu_{ij}$  and  $y_i$  denote the clean example, corresponding polluted example and the class label, respectively. Moreover,  $l_f(\cdot|\cdot)$  represents the loss function of model  $f$ .

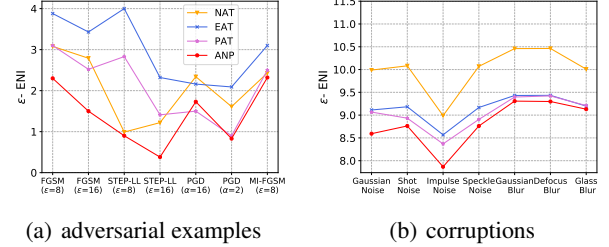


Figure 8:  $\epsilon$ -Empirical Noise Insensitivity is calculated under adversarial examples and corruptions as shown in (a) and (b).

In this section, different methods including FGSM, PGD, Gaussian noise, etc. are employed to generate adversarial and corrupted examples from 100 clean images. For each clean image, 10 corresponding polluted examples are generated with every method within noise constraint  $\epsilon$ . As shown in Figure 8 (a) and (b), ANP obtains the smallest noise insensitivity in most cases, showing the great robustness to both adversarial examples and corruptions.

Finally, more experiment results on CIFAR-10 with VGG-16 trained on ANP are shown in Figure 9. Figure 9 (a) and (b) illustrates the results on adversarial examples generated using FGSM and Step-LL with different parameters, meanwhile subfigure (c) and (d) shows the results on Gaussian noise and Shot noise.

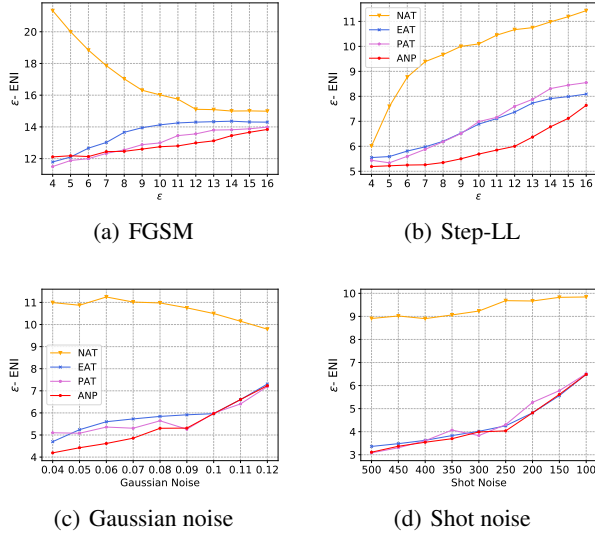


Figure 9:  $\varepsilon$ - Empirical Noise Insensitivity experiment results with adversarial examples and corrupted images generated on CIFAR-10.

### More Semantically Meaningful Gradient.

In this section, we give more experimental results of gradient visualization as shown in Figure 10. No preprocessing was applied to the gradients (other than scaling and clipping for visualization).

### How Progressive Propagation Affects Model Robustness?

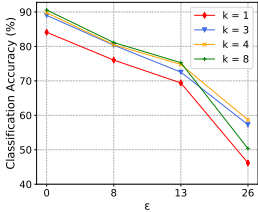


Figure 11: The effect of the progressive propagation.

and the results of the defense performance is respectively shown in Figure 11. From the figure, it is obvious that progressive procedure can improve model robustness against adversarial examples. Also, we can get insights from the view of data complexity as pointed in (Schmidt et al. 2018) that training adversarially robust model needs significantly larger sample complexity than standard model. Thus, it is understandable that the progressive propagation as well as the overall training phase improve the sample complexity which in turn promote model robustness potentially.

ANP adopts the progressive propagation to pursue the optimized noises in each layer. Here we investigate the impact of the progressive process in ANP. We train 4 VGG-16 models with different iteration number  $k$  of progressive steps. Blackbox (FGSM with different  $\varepsilon$ ) are conducted on CIFAR-10,

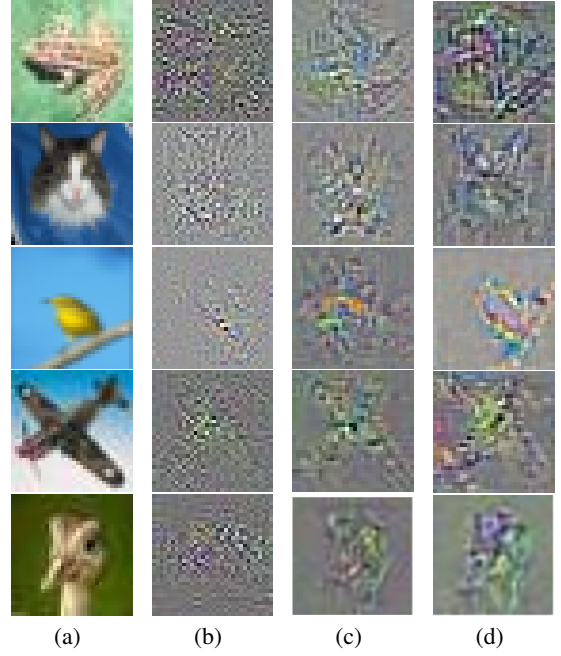


Figure 10: Visualization of the loss gradient with respect to input pixels on CIFAR-10. Subfigure (a) denotes the input image and (b) (c) and (d) represent gradients gained from Vanilla model, ANP on top-all layers and ANP on top-4 layers, respectively.

### Does Layer Depth Influence Model Robustness?

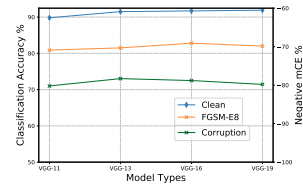


Figure 12: Deep v.s. Shallow.

low. Experimental results in Figure 12 show that the classification accuracy on clean and adversarial examples as well as negative mCE on corruption for 4 different models are nearly the same which indicates that models trained with ANP shows barely superiority between shallow and deep architectures against generalized noises.

In this section, we bring experiments for models trained by ANP with different depths, i.e., numbers of layers. We use ANP to train VGG-11, VGG-13, VGG-16 and VGG-19 with fixed hyper-parameters and test their performance on clean examples, adversarial examples and corruption, respectively.

### Hidden Representation Insensitivity.

As shown in Figure 13 (a) to (h), neurons in each layer behave more insensitively to  $\varepsilon$ -noises (PGD attack adversarial examples and corruption) after trained with ANP.

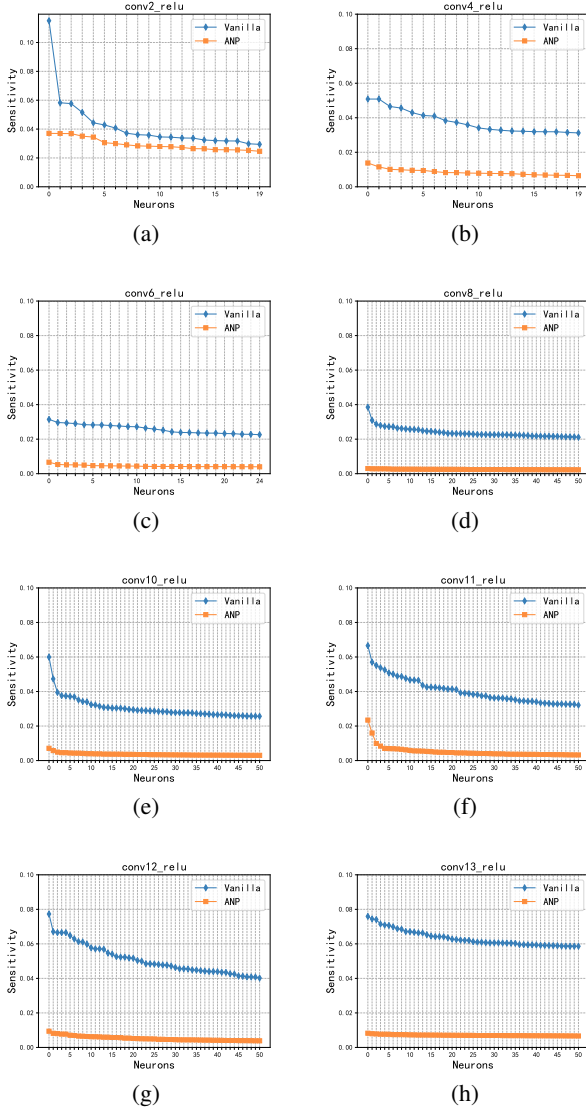


Figure 13: Hidden representation insensitivity for VGG-16 on CIFAR-10. Subfigure (a) to (h) represent the hidden representation insensitivity in layer *conv2\_relu*, *conv4\_relu*, *conv6\_relu*, *conv8\_relu*, *conv10\_relu*, *conv11\_relu*, *conv12\_relu* and *conv13\_relu*, respectively.

## Implementation Details

In this section, the implementation details of ANP and other defensive methods are given.

**ANP.** We train models with different hyper-parameters on different datasets. On MNIST, the model is trained with noises ( $\eta = 0.4$ ,  $\epsilon = 0.6$  and  $k = 8$ ). As for CIFAR-10, we first train model with clean examples for 40 epochs, then we use big noises ( $\eta = 1.0$ ,  $\epsilon = 1.0$  and  $k = 3$ ) and small noises ( $\eta = 0.3$ ,  $\epsilon = 0.3$  and  $k = 5$ ) of 50 epochs, respectively. On ImageNet, the model is trained with clean examples for 20 epochs, big noises ( $\eta = 1.0$ ,  $\epsilon = 10$  and  $k = 5$ ) for 30 epochs and 2 steps of small noises with sigum function as ( $\eta = 1.0$ ,

$\epsilon = 0.2$  and  $k = 5$ ) and ( $\eta = 0.2$ ,  $\epsilon = 0.2$  and  $k = 5$ ) for 40 epochs. During training, Gaussian noises are added to each hidden layer of the model to promote performance.

**PAT.** The adversarial examples used for PAT are generated with PGD with  $\epsilon = 8$ ,  $k = 10$  and  $\alpha = 2$  on current target model. The clean and adversarial examples in the training set are mixed in the ratio of 1 to 1.

**NAT.** The adversarial examples used for NAT are generated with Step-LL on current target model with  $\epsilon$  obeyed normal distribution  $N(0, 8)$  and truncated to  $[0, 16]$ . Moreover, the ratio of clean and adversarial examples in the training set are 1 to 1.

**EAT.** Experiment settings for EAT are the same for NAT except for the target models for adversarial example generation. On CIFAR-10, the target models are VGG-16, Inception-v2 and the current training model. Meanwhile, the target models on ImageNet are AlexNet, ResNet-18 and the current training model.

**LAT.** The noises needed at each hidden layer in current mini-batch are generated from the previous mini-batch with noise  $\epsilon$ . As the missing of detailed experiments information in the original paper, we set  $\epsilon = 0.1$  in each hidden layer.

**Rand.** On CIFAR-10, it randomly resizes input images from 32 to 36 and follows a vanilla model. However, Rand randomly resizes input images from 224 to 254 and follows an EAT trained model on ImageNet.